Prepublished copy

Nature Environment & Pollution Technology

This is a peer-reviewed prepublished version of the paper to be published in Vol. 25, No. 1, March 2026 issue

(Original Research)

Development of Zinc Oxide-Sawdust Composite Adsorbent for Methylene Blue Removal: Synthesis, Characterization, and Adsorption Mechanism

Romit Antil and Anil K. Berwal†

Centre of Excellence for Energy and Environmental Studies, Deenbandhu Chhotu Ram University of Science & Technology, Murthal, Sonipat-131039, Haryana, India

†Corresponding author: Anil K. Berwal; romit.antil2@gmail.com

Key Words	Zinc oxide-sawdust composite, Methylene blue removal, Adsorption
DOI	https://doi.org/10.46488/NEPT.2026.v25i01.B4331 (DOI will be active only after the final publication of the paper)
Citation for the Paper	Antil R. and Berwal, A.K., 2026. Development of zinc oxide-sawdust composite adsorbent for methylene blue removal: Synthesis, characterization, and adsorption mechanism. *Nature Environment and Pollution Technology*, 25(1), p. B4331. https://doi.org/10.46488/NEPT.2026.v25i01.B4331

ABSTRACT

The natural world provides sawdust, also known as wood shaving, which is a reasonably abundant and affordable lignocellulosic compound. It is a waste product of agriculture and industry that is abundant and has disposal issues. A zinc oxide nanocomposite based on sawdust (ZnO@SD) was synthesized to efficiently remove the dye methylene blue (MB) from aqueous solutions. FTIR, SEM, TEM, and XRD analyses were used to characterize the freshly made sawdust material. Batch optimization of adsorption experimental parameters, including initial dye concentration, contact time, solution pH, temperature, and adsorbent dosage used, in order to achieve the maximum removal of MB dye from wastewater. For an initial MB dye concentration of 50 mg/L, the ideal parameters for the maximum removal of MB dye from aqueous solution were determined to be: 40 mg of adsorbent, 80 minutes of contact time, a pH of 6.0 solution, and 25°C. The models that best fit the examined experimental data were Freundlich and pseudo-second order. For removal of MB dye, the experimental adsorption capacity of ZnO@SD was found to be 372.5 mg/g. According to the obtained results, the sawdust composite was thought to be an low cost and efficient adsorbent for dye removal.

1. INTRODUCTION

All the living organisms depends upon water for survival and their growth. Now a days the improved lifestyle, industrialization, as well as urbanization cause water contamination at higher rate. Water contamination has gotten worse due to a number of factors, such as the discharge of agricultural as well as domestic waste and presence of huge industrial residue in water bodies. Urbanization and industrialization have a significant impact on water quality because their effluents are highly contaminated with both organic and inorganic pollutants. As industrial sector has grown like rubber, wood, textile, and dye industries the amount of untreated wastewater that are released into stream and water bodies also increased (Yadav et al. 2023).

Among the pollutants found in wastewater, dye in particular can cause major health issues for individuals because of their carcinogenicity, mutagenicity, and toxicity even at lower concentration. These pollutants include organic dye, such as methylene blue (MB), which is present in high concentration in wastewater from a variety of industries, such as the production of paper, textiles, paint, and wool (Prodjosantoso et al. 2025). Methylene blue is a synthetic dye that is highly soluble and one of most widely used dyestuff. The MB dyestuff contributes to increased ecosystem pollution and has detrimental effects on microbes, humans, and animals (Khan et al. 2022). As it causes negative impact on the process of photosynthesis, the chemical and biological oxygen demands, and the quantities of oxygen required, which impacts the entire aquatic environment and harms human health (Ahamad and Nasar 2024). Furthermore, because of their chemical stability, they are extremely resistant to light, aerobic digestion, as well as oxidizing agent (Bo et al. 2021). As a result, wastewater treatment is crucial, and a variety of technologies, including biochemical degradation, photocatalytic, electrocoagulation, oxidative, and adsorption have been used for dye removal (Pimental et al. 2023; Dutta et al. 2021). The majority of these techniques have demonstrated their suitability in treating dye contaminated water at laboratory scales, but they have limitations when it comes to their large-scale relevance because they are expensive require a lot of energy, time, and produces large amount of secondary sludge (Bulgariu et al. 2019).

Therefore, choosing a suitable approach has always been difficult. Among the various methods, the adsorption technique has drawn a lot of interest because it is less harmful, more affordable, simpler, more flexible, and less sensitive to harmful pollutants. Additionally, this method offers adsorbent recovery and minimal sludge generation and disposal issues (Yadav et al. 2024a).

One of the recently utilized adsorbent is bio-waste and its transformation into valuable materials for specific uses. As a bio-waste from industry and agriculture, sawdust is a cheap and plentiful lignocellulosic material. In addition to different extractives (acids, soluble sugar, resins, waxes, oil, etc.), its primary constituents are cellulose, lignin, and hemicellulose. Sawdust modification enhance its ability to absorb contaminants. Therefore, various materials, such as organic compounds, basic solutions, or acidic solutions, could be used to modify it. In order to remove dyes from wastewater, metal oxide have been widely employed as promising adsorbent. Zinc oxide nanoparticle, are

used extensively in gas sensors, energy storage, and solar cells. Due to its high adsorptive capacity for a variety of pollutants, ZnO NPs attracted a lot of attention in wastewater treatment (Cao et al. 2024; Yadav et al. 2024b).

According to numerous studies, ZnO NP have shown promise as an adsorptive for organic dyes (Sayed et al. 2024). A study conducted by Zafar et al. (2019) and found that the Langmuir adsorption model and the pseudo second order rate kinetic models were used to fit the adsorption of amaranth (AM) and methyl orange (MO) onto ZnO NP. The pH of 6.0 has been found to yield the highest adsorption capacities. Zhang et al. (2016) studied that ZnO NPs demonstrated higher adsorption ability toward anionic dyes as Congo red (CR), acid fuchsin (AF) and cationic dyes malachite green (MG). For CR, AF and MG the maximum adsorption capacities were 1554mg/g, 3307mg/g, and 2963mg/g, respectively. The present study aims to synthesis ZnO NPs distributed in AC made from wood sawdust (ZnO@SD composite) for MB dye adsorption. The parameters influencing the adsorption performance including the pH of the solution, contact duration, adsorbent dosage, and initial dye concentration was thoroughly examined. Kinetic, isotherm, and thermodynamic properties were also examined.

2. MATERIALS AND METHODS

SD is used as a precursor after being gathered from nearby sawmill. Distilled water is used to wash away any contaminants that may have adhered to the wood sawdust. It is then ground and sieved after being dried for 24 hours at 100°C in an oven. Direct pyrolysis is used to produce biochar from SD and muffle furnace is used to carry out the pyrolysis process. About 20g of SD is placed in a crucible with a lid, heated for two hours at 600°C in a muffle furnace, and then allowed to cool at room temperature. After removing ash and inorganic salts with dil.HCl, the resulting biochar is cleaned in deionized water and dried at 100°C.

$ZnCl_2$ is used to chemically activate biochar, which produces activated carbon. The impregnation ratio of $ZnCl_2$ to biochar varies from 1:1. After dissolving 10 grams of $ZnCl_2$ in 150 milliliters of dissolved water, 10 grams of biochar added to mixture. Mixture was allowed to sit at room temperature for six hours. After filtering the liquid portion, the remaining solids dried in a hot oven set to 110°C for approximately 24 hours. About 10 grams of impregnated biochar are placed in a lidded crucible. ZnBC (Zinc biochar) is the name given to the activated carbon that is produced under improved operating conditions. Finally, distilled water is used to wash the biochar after it has been washed with dil.HCl until pH of filtrates reaches a constant value. After drying, the sample is stored for dye treatment in a tightly sealed container (Nirmaladevi and Palanisamy et al. 2021).

The SEM-EDS and TEM were used to examine the composite's morphological characteristics. XRD was used to determine the composite's crystalline structure. FTIR (Fourier transform infrared) spectroscopy was used to identify the composite's basic functional groups.

The adsorption models were examined using methylene blue (MB), a model organic pollutant from the Merck Group. The stock solution (1000 mg L^{-1}) prepared using 1000 mg of MB were dissolved in 1.0 L of distilled water. MB was prepared at concentrations of 100, 150, 200, 250, and 300mg L^{-1}. Using 0.010 M of NaOH and/or HCl solutions, the pH parameters of the MB solutions were brought to the expected values of 2, 4, 6, 8, and 10. A temperature-controlled shaker bath was used to hold container containing mixture of adsorbent

particle and adsorbate molecule at 25 °C. The following formula was used to determine the MB adsorption capacity q_e from the residual MB concentration:

$$\text{Adsorption efficiency (\%)} = \frac{Ci-Ce}{Ci} * 100$$

$$\text{Adsorption capacity } (q_e) = \frac{Ci-Ce}{m} * v$$

"where, V is the volume of the solution, and m is the amount of composite used.
When the adsorption tends to equilibrium, the adsorption capacity and the remaining MB concentration are indicated by q_e and C_e, respectively".

3. RESULTS AND DISCUSSION

To determine which functional groups were present on the adsorbent's surface, FTIR spectroscopy was employed (Fig.1). Cellulose and hemicellulose appear to be the primary constituents in the FTIR spectra shown in Figure 1. The FTIR spectrum revealed key functional groups in the adsorbent material. A strong absorption peak at 3354 cm^{-1} corresponds to O–H stretching vibrations of hydroxyl groups. The peak at 1745 cm^{-1} is attributed to C=O stretching from carboxylic groups in hemicellulose. A distinct band at 1516 cm^{-1} arises from –CH bending vibrations in cellulose, while the absorption at 1392 cm^{-1} is associated with C–O stretching and CH/OH bending in hemicellulose. The peak at 1039 cm^{-1} represents C–O, C–O–H, C–O–C, and ring vibrations in cellulose and hemicellulose. Finally, the band at 677 cm^{-1} suggests aromatic bending modes in cellulose (Mosoarca et al. 2021).

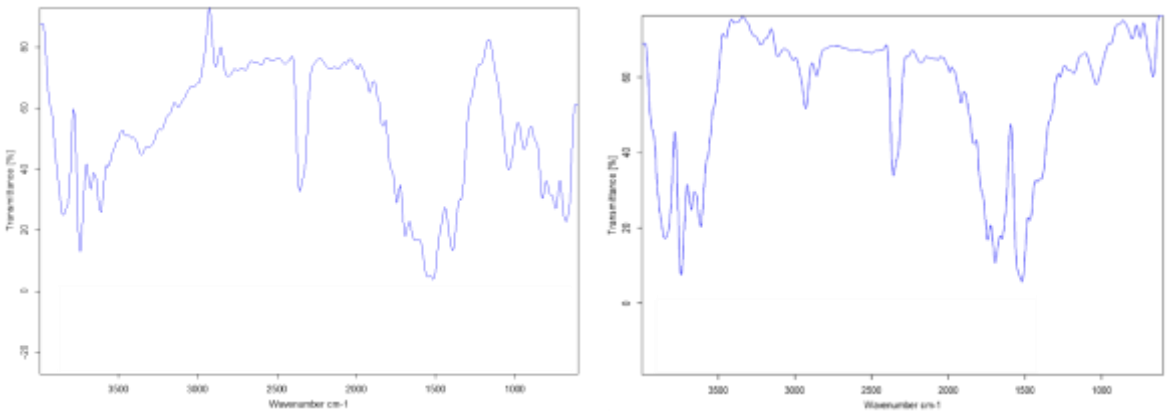

Fig. 1: FTIR spectrum of ZnO@SD before and after adsorption

The XRD result for ZnO@SD is displayed in Fig 2. Diffraction peaks were found at 32.74°, 33.49°, 36.57°, and 55.87° according to pattern analysis of the XRD. The FWHM (full full-width at half-

maximum) data result in the corresponding journals showed that the ZnO nanoparticles crystalline peaks matched the JCPDS card in the 36–1451 range. Upon closer examination, ZnO exhibits comparable properties and behavior at $20° < 2\theta < 80°$. In addition to being pure and devoid of impurities, the synthesized nano power showed no distinctive XRD peaks other than the ZnO peaks that were observed (Aigbe and Kavaz 2021).

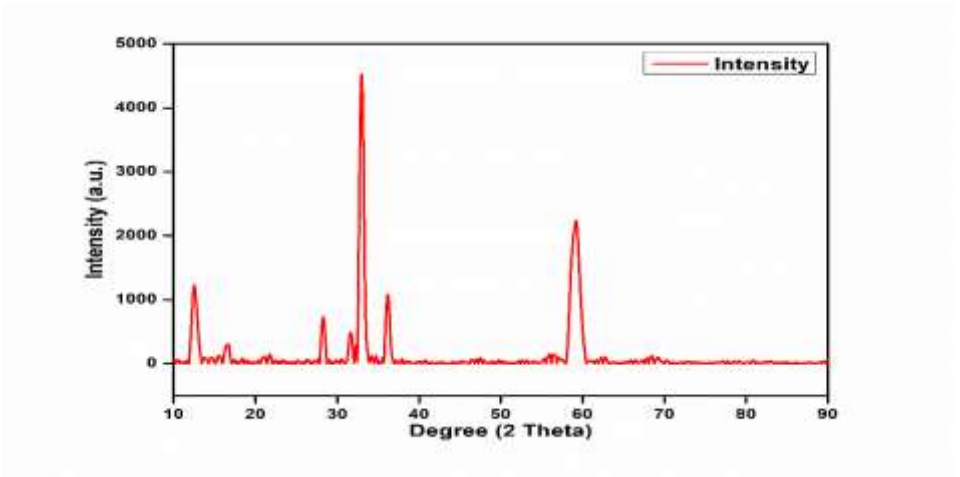

Fig. 2: XRD spectrum of ZnO@SD

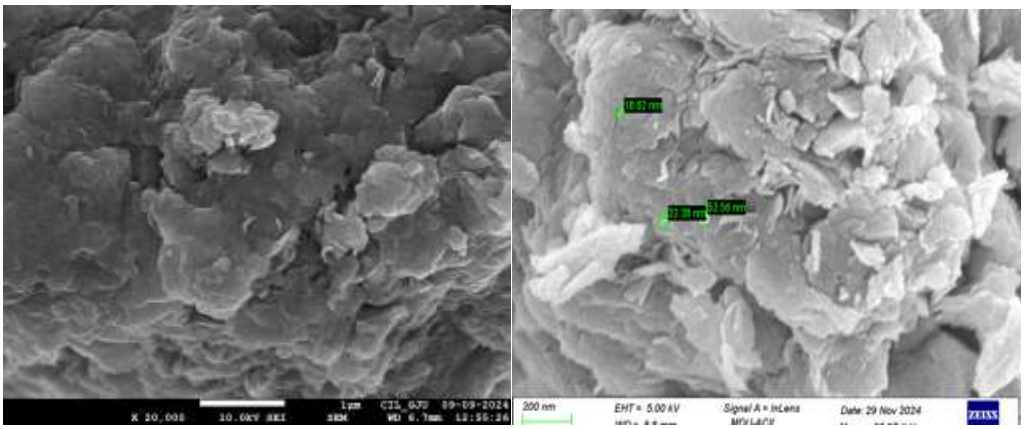

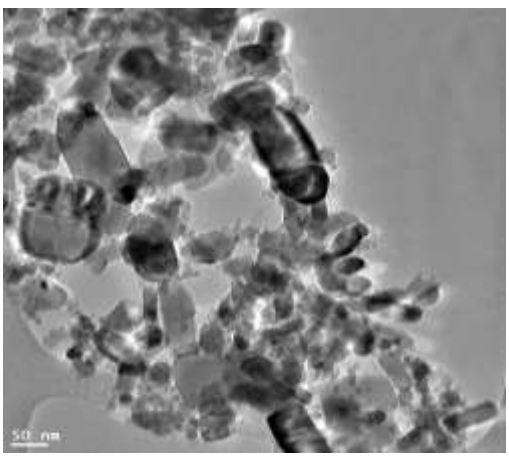

Fig. 3: SEM micrograph before and after MB adsorption; and TEM of ZnO@SD

Figure 3 displays ZnO@SD SEM images which depicts the composite were found to have fewer uniform structures. In general, it can state that the addition of carbonized-sawdust composite altered nanoparticles surface morphology. The surface, which had uniform structure and less crack became uneven. The nano-crystallites with large surface area and a strong propensity to aggregate, although the composite showed these aggregations more clearly (Aigbe et al. 2021). Multiple layers of particle arrangements are also visible, which raises the possibility of a high adsorption capacity.

The TEM image shows the porosity and surface texture of an adsorbent. There is spherical surface coverage with rough, cracked surfaces and minuscule cavities. The morphology of the particles determines which materials are suitable for adsorption. This image shows a lot of roughness and a crispy texture that could help it adsorb, and there are clearly several pores visible on the surface. Extended fibrous particles and well-formed pores appear to be the results of the porous structure. The elemental makeup of ZnO@SD nanoparticles is displayed in the EDX spectroscopy pattern in Fig. 4, which has comparable peaks for each of the samples that were characterized. The patterns showed that ZnO@SD nanoparticle had no elemental impurities and were primarily made up of these elements and their atomic percentage of Zn 8.1%, O 45.3%, and C 46.6%. The majority of organic contaminants in sawdust biomass sample seem to be broken down by carbonization. The EDX composition of ZnO@SD synthesized and after MB adsorption is displayed in Figure 4, where Zn and O were found to be the main compositional elements atomic percentage of Carbon is 73.3%, Oxygen 21.2% and Zn 1.6%.

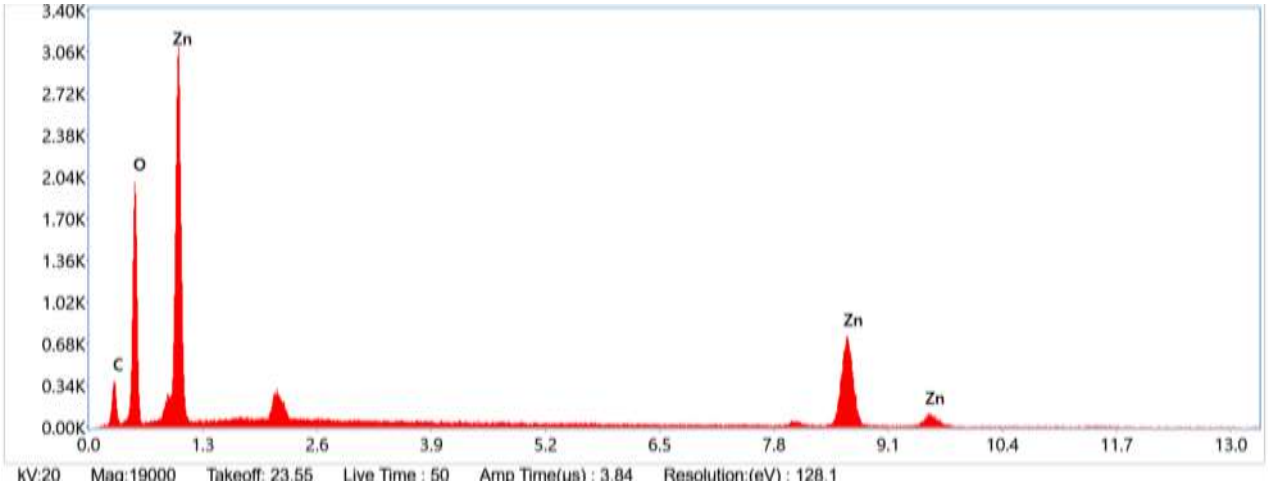

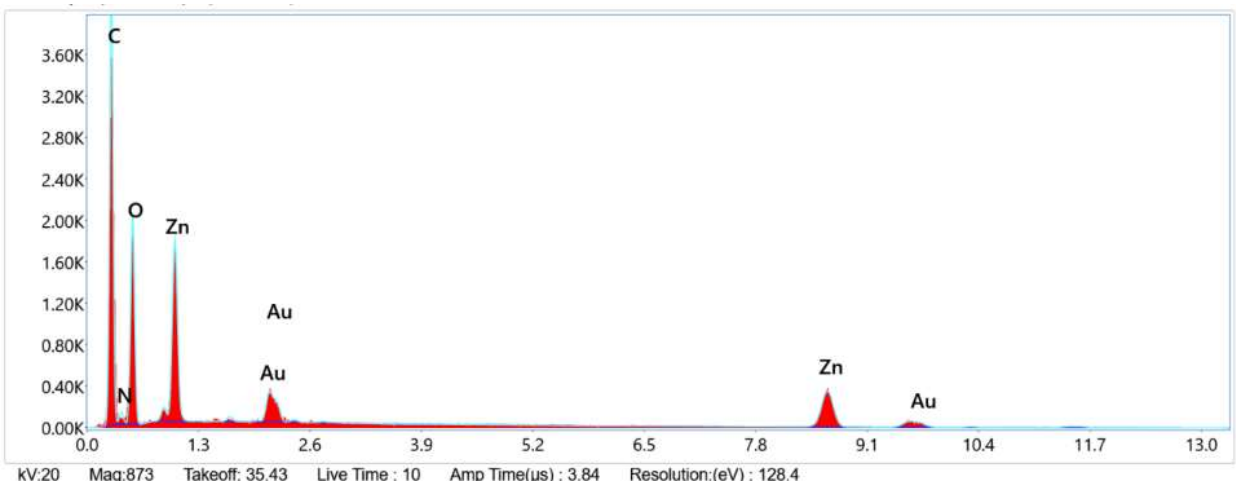

Fig. 4: EDS spectrum of ZnO@SD before and after adsorption of MB

The adsorption of MB dye to ZnO@SD is highly dependent on the composite surface charge distribution and the pH of the solution. The pH of the solution has an impact on the electrostatic interactions that are either repulsive or attractive between active sites on surface of composite and MB dye species. The impact of changing the pH of the solution on MB dye confiscation is depicted in the figure 5. It was found that the percentage of MB dye ions that were sorbed to the ZnO@SD increased significantly as the pH of the solution was changed from 2.0 to 12.0, with pH 6.0 showing the best percentage removal of MB dye ions.

As surface sites on ZnO@SD suggest that there are significantly more negatively charged groups at low pH, lower percentage of MB dye adsorbed to the ZnO@SD at pH 2 was attributed to electrostatic repulsion among negative surface charge and cationic adsorbate undissociated specie (MB). Additionally, the percentage of MB dye removed at acidic pH decreases due to increased competition among MB^+ and the H^+ and H_3O^+ ions for biochar adsorption site. At low pH values, interactions like hydrogen bonding, π-π or π+-π interaction, and porous diffusion were responsible for the removal of MB dye to the ZnO@SD (Phuong et al. 2019).

The electrostatic attraction between the dominant MB dye species (MB dye) and the dominant negatively surface charges (which rose as the pH of the solution improved) was responsible for the improved percentage of MB dye removed to the ZnO@SD. It has been reported that raising the pH of the solution increases the number of hydroxyl (-OH) and carboxylate anion (-COO-) groups on ZnO@SD surface, which in turn increases the number of negatively charged sites on the material surface (Phuong et al. 2019). Studies by Phuong et al. (2019) and Al-Ghouti and Al-Absi (2020) also revealed a similar pattern.

The primary sorption mechanisms of MB dye at acidic and basic pH are hypothesized to be electrostatic interaction and hydrogen bonding (Al-Ghouti and Al-Absi 2020; Eldeeb et al. 2024).

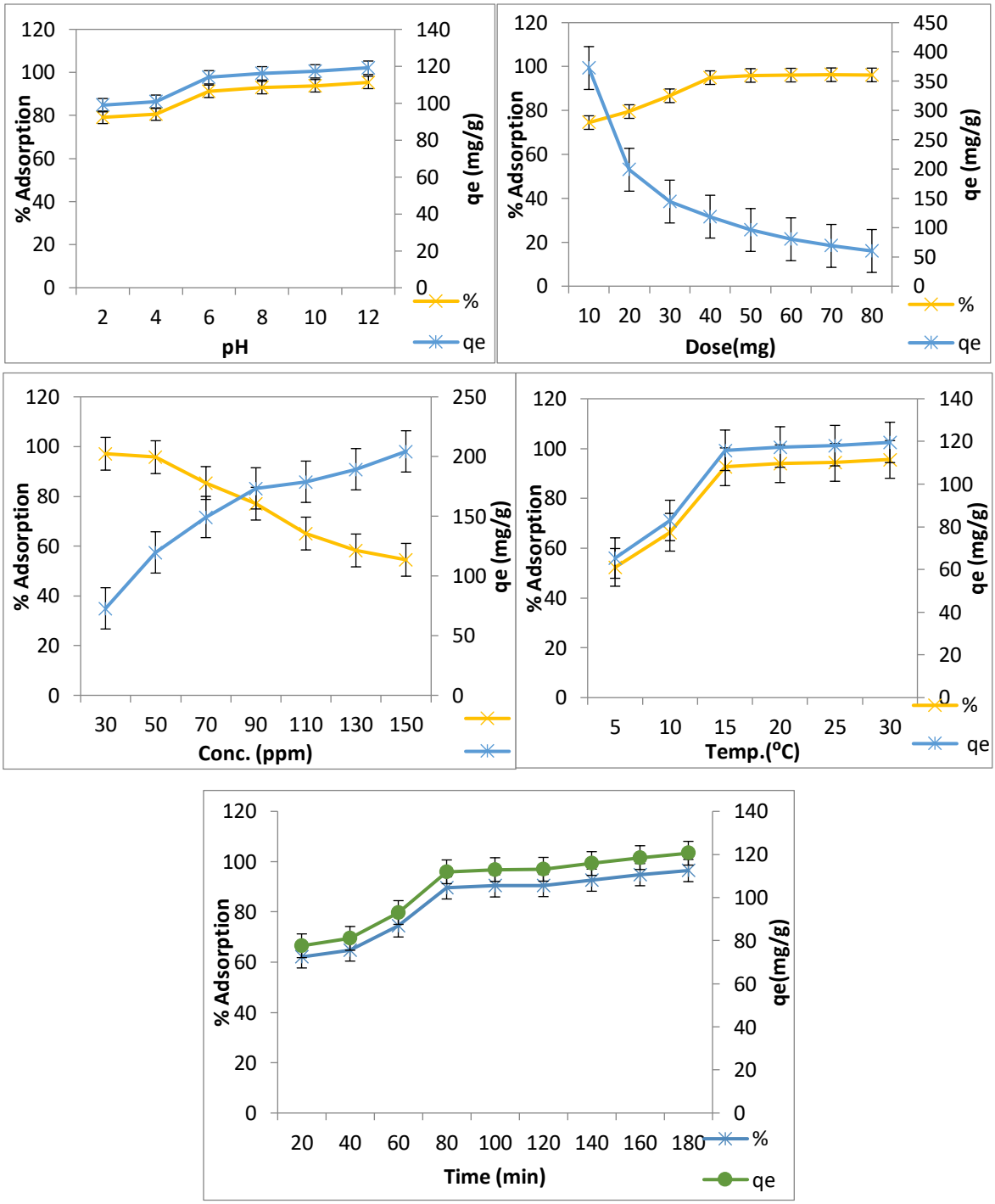

Fig. 5: Effect of pH of solution, adsorbent dosage, initial dye concentration, temperature and time on removal %age and adsorption capacity

Since it regulates the adsorption performance in the efficient removal of contaminants, the adsorbent dosage is an important parameter. The experiment used doses of ZnO@SD ranging from 10 mg to 80

mg. When the adsorbent dosage is increased from 10 mg to 70 mg, the percentage removal using ZnO@SD improves from 74.5 to 96.3% at equilibria (Fig. 5). Increased surface area and more binding sites for adsorption are the causes of the sorbate's constant improvement in percentage uptake with adsorbent dose. Nevertheless, an opposing trend in adsorption capacity was noted, as shown in Fig 5. The maximum adsorption capacity of 372.5 mg g^{-1} for M.B. by adsorbent was noted at the lowest adsorbent dose. In light of this, it is important to note that adsorbent particles interact through amalgamation and aggregation at higher doses, resulting in a decrease in effective surface area per unit weight of adsorbent. It could be explained by an increase in the adsorbent's surface area and an enhancement in accessibility of more active surface site on sorbent (Garg et al. 2004). On the other hand, as the dose is increased, the adsorption capacity continuously and significantly decreases. Adsorbent particle interactions such as agglomeration and aggregation cause adsorption-capacity to decrease as sorbent dose increases. As a result, the adsorbents total surface area per unit weight decreases.

Methylene Blue (MB) dye adsorption tests were performed at various contact duration ranging from 20 to 180 minute with initial MB concentration of 50 ppm to examine the adsorption kinetics. The effects of contact time on adsorption efficiency were examined at 298 K, 40 mg, and 6 pH. As contact time increased to 80 minutes removal %age rose to 89.56%, and the adsorption finally reached equilibrium. The figure 5 shows how initial MB concentration affected adsorption efficiency. There were sporadic variations in curves of different starting concentration. As MB concentration ranging from 10 to 150 mg L^{-1}, the highest adsorption efficiency of 97.13% at 30 ppm was noted.

The persistent active sites found it difficult to bind up the rising MB molecule from bulk phase, even though there were enough active sites to explain the results at low initial MB dye concentrations. At higher methylene blue (MB) concentrations, increased electrostatic repulsion between dye cations can reduce adsorption efficiency. However, elevating the initial MB concentration also enhances the adsorption capacity of the ZnO@SD composite. This occurs because a higher dye concentration provides a stronger driving force, helping to overcome mass transfer resistance between the aqueous phase and the adsorbent surface (Hassaan et al., 2023).

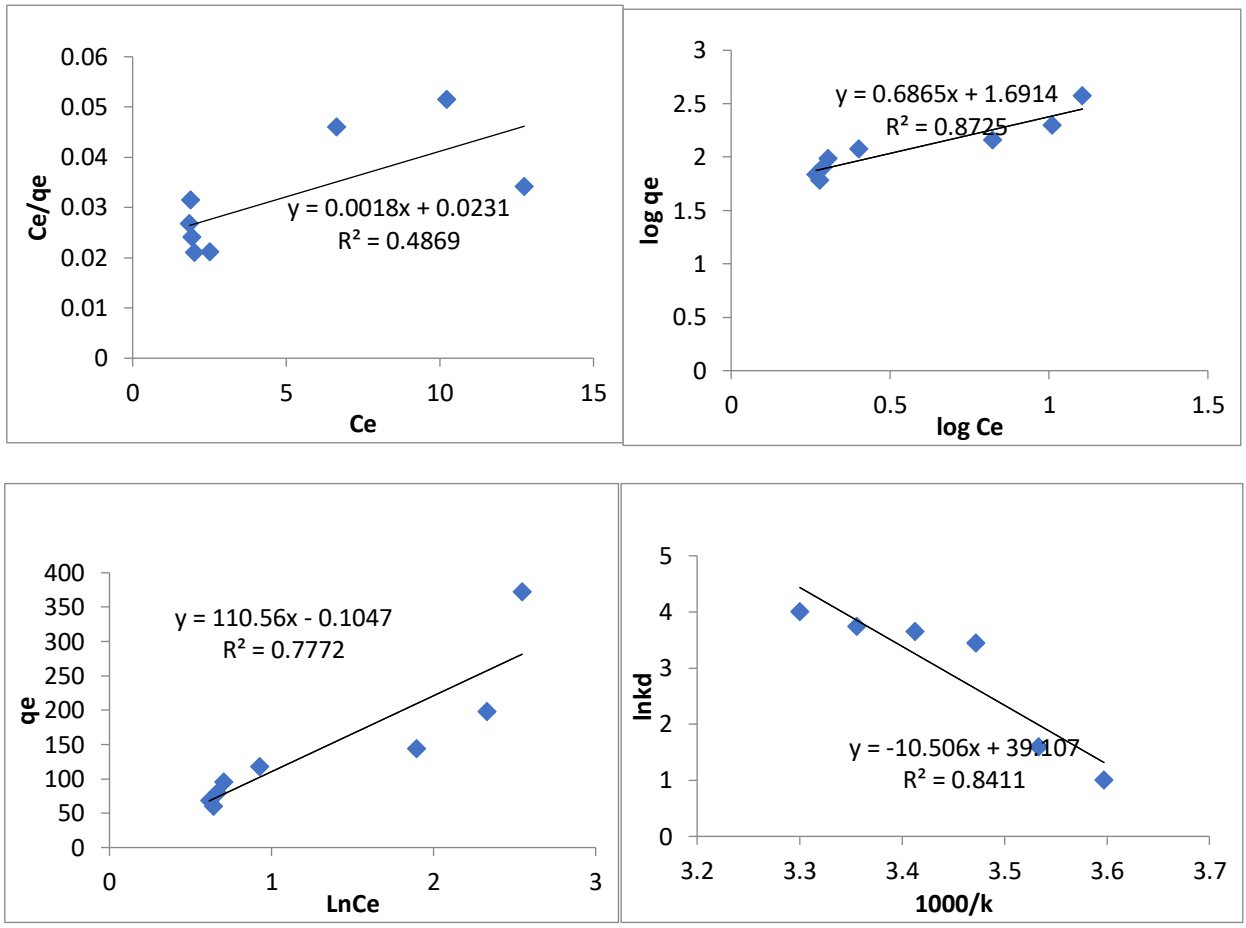

Fig. 6: Isotherms: Langmuir, Freundlich and Temkin; and Vant hoff plot

Adsorption isotherm modeling can be used to justify interaction of dye molecule with sorbent in solid/liquid interfaces. Three isotherm models the Langmuir, Freundlich, and Temkin models were applied to the experimental data of dye adsorption at different dye concentrations (10–150 mg L^{-1}). The Langmuir isotherm model is based on the assumption that adsorption occurs in a monolayer, where dye molecules bind to a finite number of identical and energetically equivalent active sites on the adsorbent surface. This model also presumes that no interactions occur between adsorbed molecules (Langmuir 1916). In contrast, the Freundlich isotherm model is an empirical equation that describes multilayer adsorption on a heterogeneous surface with non-uniform binding sites. Unlike the Langmuir model, it does not assume a saturation limit, implying an infinite number of active sites with varying adsorption energies (Freundlich 1906). According to the Temkin model, adsorbate's heat energy decreases linearly with monolayer coverage. The surface has an even distribution of active binding-sites (Temkin and Pyzhev 1940). The models' linear plots are displayed in Fig. 6. Table 1 summarizes the results of the calculation of each model's regression coefficient and isotherm model parameter using the corresponding

linear plots. Each model's regression coefficient and isotherm parameters were used to determine how applicable it was to dye adsorption experiments. The results of a comparison revealed that the Freundlich model best described the MB dye adsorption process. It shows that MB dye molecules have been adsorbed in multiple layers onto the heterogeneous surface-active sites.

For MB dye, the Freundlich model's R^2 was determined to be 0.87. The fact that 1/n (slope) values ranged from 0 to 1, or 0.686 for MB, suggests that adsorption was advantageous and that dye molecules chemically bonded to adsorbent surface is chemisorption. A value of 1/n less than 1 indicates chemisorption on the adsorbents heterogeneous surface. The MB dye's R_L value was found to be between 0.206 ($0 < R_L > 1$), confirming a favorable adsorption process. It was discovered that MB dye had a maximum monolayer adsorption capacity (q_m) of 555.5 mg g^{-1} but the experimental is 372.5mg g^{-1}. Consequently, the chemisorption of dye molecules onto Zn@SD was validated by the isothermic models. Temperature ranges of 278–303 K were examined because thermodynamic research offers more details regarding adsorption mechanism of ZnO@SD on MB. The van't Hoff equation was used to calculate all thermodynamic parameter, including enthalpy (ΔH), entropy change (ΔS), and the standard Gibbs free energy (ΔG), which showed how the equilibrium constant depended on temperature. The equilibrium constant (K) was determined from the adsorption isotherm data using the following equation:

$K = q_e/C_e$, While the positive value of ΔS° 0.325KJ/mol/K showed that the randomness at solid/solution interface increased, and positive value of enthalpy ΔH° 87.29 KJ/mol/K, which is one of the thermodynamic parameters shown in Table 1, confirmed that adsorption of MB onto ZnO@SD was endothermic in nature. This was because the adsorbate ions lost less transitional energy than the water molecules that were displaced by the adsorbate species. The adsorption mechanism of MB onto the ZnO@SD nanocomposite was a favorable spontaneous process, as indicated by the negative values of ΔG°. Enthalpy ΔH°<84 kJ/mol indicates physisorption, while values between 84 and 420 kJ/mol indicate chemisorption, according to current study it is 87.29 means chemisorption, it is on the borderline between physisorption and chemisorption. The possibility of multilayer adsorption or pore-filling mechanisms (physisorption). The potential involvement of strong chemical interaction (ligand exchange, complexation) supporting chemisorption. The influence of temperature on adsorption mechanism, as higher ΔH° values often correlate with chemisorption but may also reflect high-energy physical

adsorption. Consequently, it suggests that a chemical interaction may be the mechanism underlying sorption of MB onto ZnO@SD.

Table 1: Isotherms, thermodynamics and kinetics

	Parameters	Values
Langmuir	q_m	555.5
	B	0.077
	R_L	0.206
	R^2	0.48
Freundlich	1/n	0.686
	K_f	48.97
	R^2	0.87
Temkin	A_T	1.00
	R^2	0.77
Thermodynamics	ΔS˚	0.325
	ΔH˚	87.29
	ΔG˚ 278K	-1.67
	ΔG˚283K	-3.27
	ΔG˚288K	-4.87
	ΔG˚293K	-6.47
	ΔG˚298K	-8.07
	ΔG˚303K	-9.67
PFO	q_e	1.01
	K1	3.89
	R^2	0.87
PSO	q_e	133.33
	K2	0.00037
	R^2	0.99

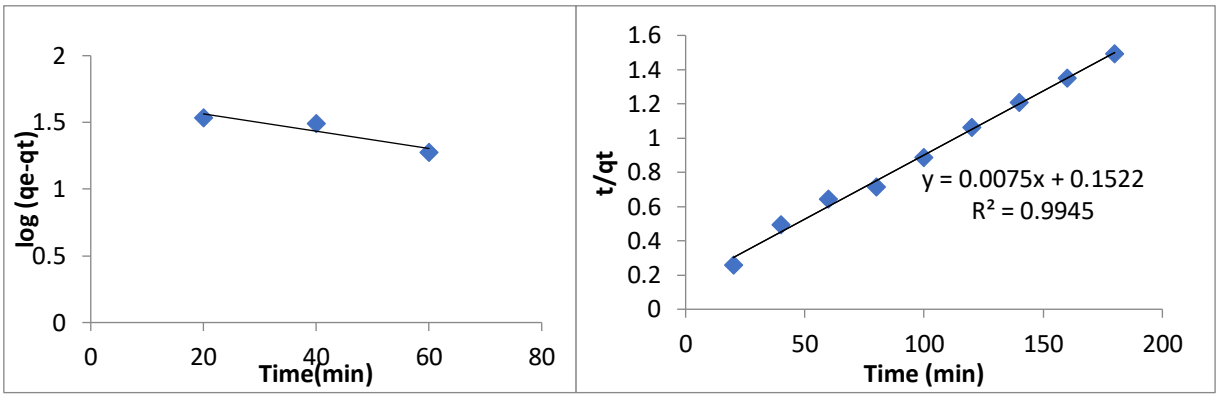

Fig. 7: Kinetics study

Pseudo first order rate kinetics and pseudo second order rate kinetic model were used to further study adsorption phenomenon, and Table 1 summarizes the parameters that were obtained: Table 1 shows that kinetics of MB adsorption onto ZnO@SD nanocomposite are described by pseudo second order rate kinetics model. In comparison to the pseudo-first-order model, the linear regression values derived from this model yielded a higher correlation coefficient (R^2) of >0.99. The model's suitability for describing the adsorption process is further supported by the observation of linear curves in Figure 7, which also shows fitment to pseudo second order. It's possible that methylene blue interaction with adsorption site was chemical in nature because adsorption process adheres to the pseudo-second-order model.

It was proposed that chemical adsorption played a role in achieving the highest MB adsorption from simulated water, given the scale used in linearized form of pseudo-second-order model. Pseudo-second-order kinetics was also used to model the early stage of kinetic experimental data in order to verify this (Figure 7). Based on this evidence, the adsorption kinetics of MB onto ZnO@SD nanocomposite are primarily diffusion based mechanisms. During a rate-limiting mechanistic step, various adsorption sites on a homogeneous solid substrate randomly collide with one another and diffuse through the adsorbent pore size.

4. CONCLUSIONS

Sawdust is a cheap and plentiful lignocellulosic material that is a bio-waste product of industry and agriculture. In this study, mixed sawdust was used as the raw material to produce ZnO@SD adsorbent. ZnO@SD has a network structure and works well as an adsorbent for cationic dyes because it has a lot of amino, hydroxyl, and carboxyl groups. ZnO@SD can be used to adsorb cationic dye MB in water and has a favorable separation capacity, high removal rate, good adsorption capacity. The aforementioned processes are well-fitted by the Freundlich adsorption isotherm and the pseudo-second-order kinetic model. ZnO@SD's easy preparation method and superior adsorption

capabilities, this work offers useful ZnO@SD adsorbents for the elimination of cationic dyes from wastewater. It is a low-cost bio-waste sawdust, which is a sustainable, scalable, and environmentally friendly method can show great promise for a variety of additional uses in the future.

Author Contributions: For research articles with multiple authors, include a brief paragraph outlining each author's contributions using the following format: "Conceptualization, R.A. and A.K.B.; methodology, R.A.; software, R.A..; validation, A.K.B.; formal analysis, R.A.; investigation, A.K.B.; resources, R.A.; data curation, R.A.; writing—original draft preparation, R.A.; writing—review and editing, A.K.B.; visualization, R.A.; supervision, A.K.B.; project administration, A.K.B. All authors have read and agreed to the published version of the manuscript." Authorship should be restricted to individuals who have made significant contributions to the research.

Acknowledgments: The authors are thankful to DCRUST, Murthal.

Conflicts of Interest: "The authors declare no conflicts of interest."

REFERENCES

1. Ahamad, Z., & Nasar, A. 2024. Synthesis, characterization, and application of magnetized Azadirachta indica sawdust as a novel adsorbent: kinetic, and isotherm studies in removing methylene blue as a model dye. *Cellulose*, *31*(6), 3763-3782.
2. Aigbe, R., & Kavaz, D. 2021. Unravel the potential of zinc oxide nanoparticle-carbonized sawdust matrix for removal of lead (II) ions from aqueous solution. *Chinese Journal of Chemical Engineering*, *29*, 92-102.
3. Aigbe, R., Akhayere, E., Kavaz, D., & Akiode, O. K. 2021. Characteristics of zinc oxide and carbonized sawdust nanocomposite in the removal of cadmium (II) ions from water. *Water, Air, & Soil Pollution*, *232*, 1-19.
4. Al-Ghouti, M. A., & Al-Absi, R. S. 2020. Mechanistic understanding of the adsorption and thermodynamic aspects of cationic methylene blue dye onto cellulosic olive stones biomass from wastewater. *Scientific Reports*, *10*(1), 15928.
5. Bo, L., Gao, F., Bian, Y., Liu, Z., & Dai, Y. 2021. A novel adsorbent Auricularia Auricular for the removal of methylene blue from aqueous solution: Isotherm and kinetics studies. *Environmental Technology & Innovation*, *23*, 101576.
6. Bulgariu, L., Escudero, L. B., Bello, O. S., Iqbal, M., Nisar, J., Adegoke, K. A., & Anastopoulos, I. 2019. The utilization of leaf-based adsorbents for dyes removal: A review. *Journal of Molecular Liquids*, *276*, 728-747.
7. Cao, V., Cao, P.A., Han, D.L., Ngo, M.T., Vuong, T.X. and Manh, H.N., 2024. The suitability of Fe3O4/graphene oxide nanocomposite for adsorptive removal of methylene blue and congo red. Nature Environment and Pollution Technology, 23(1), pp.255-263. 10.46488/NEPT.2024.v23i01.021
8. Dutta, S., Gupta, B., Srivastava, S. K., & Gupta, A. K. 2021. Recent advances on the removal of dyes from wastewater using various adsorbents: A critical review. *Materials Advances*, *2*(14), 4497-4531.

9. Eldeeb, T. M., Aigbe, U. O., Ukhurebor, K. E., Onyancha, R. B., El-Nemr, M. A., Hassaan, M. A., & El Nemr, A. 2024. Adsorption of methylene blue (MB) dye on ozone, purified and sonicated sawdust biochars. *Biomass Conversion and Biorefinery*, *14*(8), 9361-9383.
10. Freundlich, H. M. F. 1906. Over the adsorption in solution. *J. Phys. chem*, *57*(385471), 1100-1107.
11. Garg, V. K., Amita, M., Kumar, R., & Gupta, R. 2004. Basic dye (methylene blue) removal from simulated wastewater by adsorption using Indian Rosewood sawdust: a timber industry waste. *Dyes and pigments*, *63*(3), 243-250.
12. Hassaan, M. A., Yılmaz, M., Helal, M., A., M., Ragab, S., & El Nemr, A. 2023. Isotherm and kinetic investigations of sawdust-based biochar modified by ammonia to remove methylene blue from water. *Scientific Reports*, *13*(1), 1-20. https://doi.org/10.1038/s41598-023-39971-0
13. Khan, I., Saeed, K., Zekker, I., Zhang, B., Hendi, A. H., Ahmad, A., & Khan, I. 2022. Review on methylene blue: Its properties, uses, toxicity and photodegradation. *Water*, *14*(2), 242.
14. Langmuir, I. 1916. The constitution and fundamental properties of solids and liquids. Part I. Solids. *Journal of the American chemical society*, *38*(11), 2221-2295.
15. Mosoarca, G., Popa, S., Vancea, C., & Boran, S. 2020. Optimization, Equilibrium and Kinetic Modeling of Methylene Blue Removal from Aqueous Solutions Using Dry Bean Pods Husks Powder. *Materials*, *14*(19), 5673. https://doi.org/10.3390/ma14195673
16. Nirmaladevi, S., & Palanisamy, P. N. 2021. Adsorptive behavior of biochar and zinc chloride activated hydrochar prepared from Acacia leucophloea wood sawdust: kinetic equilibrium and thermodynamic studies. *Desalination Water Treat*, *209*, 170-181.
17. Phuong, D. T. M., Loc, N. X., & Miyanishi, T. 2019. Efficiency of dye adsorption by biochars produced from residues of two rice varieties, Japanese Koshihikari and Vietnamese IR50404. *Desalin. Water Treat*, *165*, 333-351.
18. Pimentel, C. H., Freire, M. S., Gómez-Díaz, D., & González-Álvarez, J. 2023. Preparation of activated carbon from pine (Pinus radiata) sawdust by chemical activation with zinc chloride for wood dye adsorption. *Biomass Conversion and Biorefinery*, *13*(18), 16537-16555.
19. Prodjosantoso, A.K., Nurul Hanifah, T.K., Utomo, M.P., Budimarwanti, C. and Sari, L.P., 2025. The Synthesis of AgNPs/SAC Using Banana Frond Extract as a Bioreducing Agent and its Application as Photocatalyst in Methylene Blue Degradation. Nature Environment & Pollution Technology, 24(1). 10.46488/NEPT.2025.v24i01.D1688

20. Sayed, N. S., Ahmed, A. S., Abdallah, M. H., & Gouda, G. A. 2024. ZnO@ activated carbon derived from wood sawdust as adsorbent for removal of methyl red and methyl orange from aqueous solutions. *Scientific Reports*, *14*(1), 1-18. https://doi.org/10.1038/s41598-024-55158-7
21. Temkin, M. J., & Pyzhev, V. 1940. Recent modifications to Langmuir isotherms.
22. Yadav, S., Bajar, S., Hemraj et al. 2023. Assessment of groundwater quality near municipal solid waste landfill by using multivariate statistical technique and GIS: a case study of Bandhwari (Gurugram) landfill site, Haryana, India. *Sustain. Water Resour. Manag.* 9, 174 (2023)
23. Yadav, S., Rohilla, R. & Chhikara, S.K. 2024a. Review on Landfill Leachate Treatment: Focus on the Applicability of Adsorbents. *Proc. Natl. Acad. Sci., India, Sect. B Biol. Sci.*
24. Yadav, S., Yadav, A., Goyal,G., Dhawan, M., Kumar, V., Yadav, A., Dhankhar, R., Sehrawat, N., Chhikara, SK. 2024b. Fly Ash-based Adsorption for Hexavalent Chromium Removal in Aqueous Systems: A Promising Eco-Friendly Technique. *Oriental Journal of Chemistry,* 40 (1), 182
25. Zafar, M. N., Dar, Q., Nawaz, F., Zafar, M. N., Iqbal, M., & Nazar, M. F. 2019. Effective adsorptive removal of azo dyes over spherical ZnO nanoparticles. *Journal of Materials Research and Technology*, *8*(1), 713-725.
26. Zhang, F., Chen, X., Wu, F., & Ji, Y. 2016. High adsorption capability and selectivity of ZnO nanoparticles for dye removal. *Colloids and Surfaces A: Physicochemical and Engineering Aspects*, *509*, 474-483.